J-STAGE Advance Publication: July 9, 2018
Journal of Oral Science

Original

Effect of a coating material containing surface reaction-type pre-reacted glass-ionomer filler on prevention of primary enamel demineralization detected by optical coherence tomography

Ryosuke Murayama[1)], Yuko Nagura[2)], Kabun Yamauchi[2)], Nobuyuki Moritake[2)], Masayoshi Iino[1)], Ryo Ishii[1)], Hiroyasu Kurokawa[1)], Masashi Miyazaki[1)], and Yumiko Hosoya[1,3)]

[1)]Department of Operative Dentistry, Nihon University School of Dentistry, Tokyo, Japan
[2)]Division of Applied Oral Sciences, Nihon University Graduate School of Dentistry, Tokyo, Japan
[3)]Hosoya General Incorporated Association, Chiba, Japan

(Received July 10, 2017; Accepted October 23, 2017)

Abstract: We used optical coherence tomography to examine the effect of a coating material containing surface reaction-type pre-reacted glass-ionomer (S-PRG) filler on primary enamel demineralization in 18 extracted human primary teeth. The pulp was removed, and each tooth was ultrasonically cleaned with distilled water. Six teeth were treated with 0.1-M lactic acid buffer solution (De group). In the second group (n = 6), a thin film of coating material was applied before demineralization (PRG group). A third group (Control group; n = 6) was maintained in artificial saliva. Using optical coherence tomography, we measured peak signal intensity (dB) and width at $1/e^2$ (μm) at predetermined locations on the enamel surface and calculated integrated values. All data were analyzed with ANOVA and the Tukey-Kramer test ($\alpha = 0.05$). Although changes in integrated values differed between groups, there was a small but significant increase in the Control group and a small but significant decrease in the De group. In the PRG group, integrated values were significantly higher at 7 days after the start of the experiment and significantly increased thereafter. Our findings indicate that a coating material containing S-PRG fillers may prevent primary enamel demineralization.

Keywords: enamel; demineralization; optical coherence tomography; S-PRG filler; coating material.

Introduction

Although the incidence of caries in primary dentition has declined, not all children have benefited equally. The frequency of early childhood caries, and more typical primary caries in young children with low socioeconomic status, remains considerable, and the number of untreated primary teeth with carious lesions in these children is high (1,2). Early oral examinations and preventive and restorative dental treatments are crucial in combating dental diseases in young populations (3). The marked increase in caries risk among young children highlights the need for optimized caries-preventive regimens and innovative preventive techniques (4). Treatment to arrest caries is also useful for treating incipient lesions in teeth that have not fully erupted and are immaturely mineralized. Systemic and topical fluoride has reduced caries incidence in primary and permanent dentition (5). Recently, a new fluoride-releasing coating material containing a

Correspondence to Dr. Masashi Miyazaki, Department of Operative Dentistry, Nihon University School of Dentistry, 1-8-13 Kanda-Surugadai, Chiyoda-ku, Tokyo 101-8310, Japan
Fax: +81-3-3219-8347 E-mail: miyazaki.masashi@nihon-u.ac.jp

Color figures can be viewed in the online issue at J-STAGE.
doi.org/10.2334/josnusd.17-0256
DN/JST.JSTAGE/josnusd/17-0256

Table 1 The surface reaction-type pre-reacted glass-ionomer varnish used in this study

	Ingredients
Base	S-PRG filler (mean diameter, 3.0 μm), distilled water, methacrylic acid monomer, others
Active	Phosphonic acid monomer, methacrylic acid monomer, bis-MPEPP, carboxylic monomer, TEGDMA, initiator, others

S-PRG: surface reaction-type pre-reacted glass ionomer; bis-MPEPP: 2,2'-bis(4-methacryloxy polyethoxyphenyl) propane; TEGDMA: triethylene glycol dimethacrylate.

surface reaction-type pre-reacted glass-ionomer (S-PRG) filler was introduced for use in caries prevention and may help enhance mineralization and reduce acidic attack by oral cariogenic bacteria (6,7).

S-PRG fillers are prepared via an acid-base reaction between fluoroaluminosilicate glass powder and polyacrylic acidic solution, which forms a stable glass-ionomer phase on a glass filler surface (8). A ligand exchange mechanism within the pre-reacted hydrogel enables S-PRG fillers to release and recharge fluoride (9). In addition to fluoride ions, S-PRG fillers release ions such as SiO_3^{2-}, Sr^{2+}, Al^{3+}, BO_3^{3-}, and Na^+ (10,11). Fluoride and silicate induce pronounced remineralization of the tooth substrate, thus repairing incipient lesions (12). Strontium and fluoride also improve acid resistance of teeth by converting hydroxyapatite to strontium-apatite and fluoroapatite (13). When S-PRG filler comes into contact with acids, it can change the pH of solutions to within a weakly alkaline range (14). Coating materials containing S-PRG filler can flatten the tooth surface and protect against bacterial retention in incipient caries (15,16). However, few studies have evaluated the effects of coating materials containing S-PRG filler as a caries-preventive treatment for primary tooth enamel.

Numerous diagnostic techniques have recently been developed to detect demineralization and remineralization during formation of carious lesions (17). Optical coherence tomography (OCT), a diagnostic technique for obtaining cross-sectional images of the internal structure of lesions, has considerable potential for noninvasive imaging of demineralizing lesions, because it obviates the need to remove the surface and eliminates radiation exposure (18,19). In the detection of re- and de-mineralization, the mechanisms of OCT differ from those of transverse microradiography, the standard method for assessing mineral changes in experimental lesions of teeth.

In this study, we used OCT to examine the effects of a coating material containing S-PRG filler on changes in the structure of artificially demineralized primary tooth enamel. The null hypothesis tested was that the coating material would not affect the structural condition of artificially demineralized primary tooth enamel.

Materials and Methods

Eighteen healthy primary teeth (nine primary canines and nine primary molars) that were extracted to expedite eruption of permanent teeth or for orthodontic reasons were used as substrates for this study. Informed consent for tooth collection was obtained from parents and patients, in accordance with the regulations of the Ethical Committee of Nihon University School of Dentistry, Tokyo, Japan (EP2008-19). The teeth were frozen in physiologic saline within 10 min of extraction.

After separating the root with a low-speed diamond saw (IsoMet 1000; Buehler Ltd., Lake Bluff, IL, USA), the pulp was removed, and each tooth was ultrasonically cleaned in distilled water. The enamel surfaces of the teeth, excluding the labial surfaces of primary canines and buccal and lingual surfaces of primary molars, were coated with a light-cured varnish intended to enhance intraoral health by controlling areas at high risk of caries. The composition of the varnish, which contained S-PRG filler (PRG Barrier Coat; Shofu Inc., Kyoto, Japan), is shown in Table 1.

One group of six specimens was treated with a demineralizing solution containing undersaturated 0.1-M lactic acid buffer solution (pH 4.75; 0.75 mM $CaCl_2$•$2H_2O$ and 0.45 mM KH_2PO_4) for 30 min and then placed in artificial saliva (pH 7.0; 14.4 mM NaCl, 16.1 mM KCl, 0.3 mM $MgCl_2$•$6H_2O$, 2 mM KH_2PO_4, 1 mM $CaCl_2$•$2H_2O$, and 0.1 g/100 mL sodium carboxymethyl cellulose; De group). These procedures were conducted twice daily throughout the 4-week test period, and the specimens were maintained in artificial saliva at 37°C between treatments. For the specimens in the second group, a thin film of the coating material containing S-PRG filler was applied. The specimens were then light-irradiated for 10 s with a curing unit (Optilux 501; Kerr, Orange, CA, USA) before treatment with the demineralizing solution (PRG group). Specimens in the third group were maintained in artificial saliva for the same time period (Control group), as shown in Fig. 1.

The present OCT system (J. Morita Tokyo Mfg. Corp., Saitama, Japan) and methods for data correction were described in a previous report (20). A scanning probe connected to the OCT device was fixed 2 mm from the

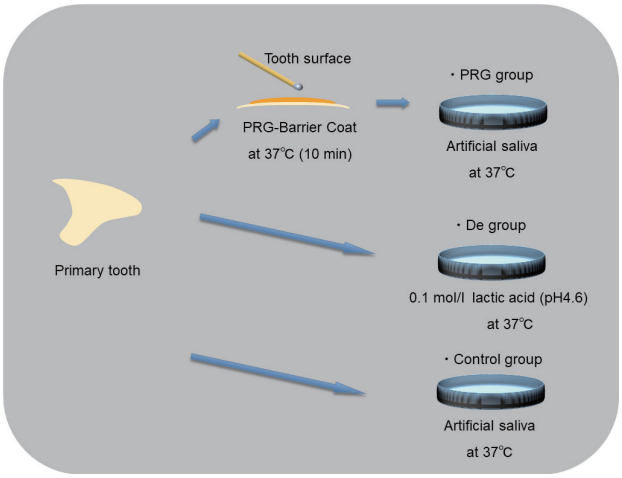

Fig. 1 Experimental protocol of the present study.

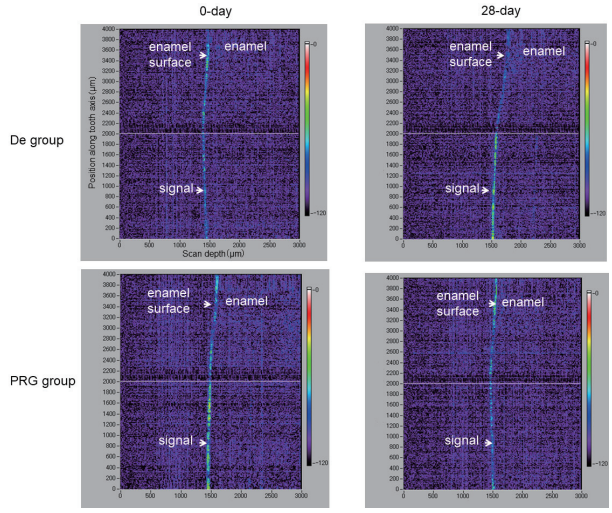

Fig. 2 Representative B-scan images of enamel surfaces of the De and PRG groups. The x-axis of each tomogram shows scan depth, and the y-axis shows the vertical measurement position at the tooth surface. In the De group, a weak, narrow signal without back-scattered intensity was observed on Day 0, with little change in optical coherence tomography images during the test period. In contrast, signal intensities in the PRG group weakened after the 28-day storage period.

Table 2 Effect of treatment procedure and duration on signal intensity (dB)

	Treatment duration (days)				
Group	0	7	14	21	28
Control	−47.1 (6.3) aA	−47.7 (5.4) aA	−47.1 (4.9) aA	−47.6 (5.1) aA	−47.9 (5.2) aA
De	−49.1 (5.6) aA	−39.6 (7.4) bA	−36.7 (5.7) bA	−36.7 (5.9) bA	−38.3 (5.6) bA
PRG	−47.2 (5.1) aA	−62.8 (6.6) bcB	−65.1 (7.3) bcB	−66.7 (7.6) bcB	−73.8 (5.5) cB

De, Demineralization group; PRG: PRG filler extraction solution. Data are means (standard deviation). $n = 6$ per group. Values in the same group with the same lowercase letters indicate no significant difference ($P > 0.05$). For values in different groups at the same treatment time, means with the same uppercase letters are not significantly different ($P > 0.05$).

Table 3 Effect of treatment procedure and duration on width at $1/e^2$ (μm)

	Treatment time (days)				
Group	0	7	14	21	28
Control	80 (11.6) aA	80 (11.6) aA	80 (10.0) aA	80 (13.3) aA	80 (13.3) aA
De	80 (13.3) aA	70 (13.3) aA	70 (10.0) aA	70 (10.0) aA	70 (13.3) aA
PRG	80 (11.6) aA	110 (11.6) bB	180 (13.3) cB	180 (13.3) cB	180 (15.0) cB

De, Demineralization group; PRG, PRG filler extraction solution. Data are means (standard deviation). $n = 6$ per group. Values in the same group with the same lowercase letters indicate no significant difference ($P > 0.05$). For values in different groups at the same treatment time, means with the same uppercase letters are not significantly different ($P > 0.05$).

treated enamel surface, and the width between points where intensity decreased to a value of $1/e^2$ was calculated (21). Calculation of the integrated value (dB·μm) was based on the area of peak intensity as determined by OCT.

The data for each group were analyzed by repeated-measures analysis of variance followed by the Tukey-Kramer *post-hoc* multiple-comparisons test, with a significance level of 0.05. Statistical analysis was performed with commercial statistical software (SigmaPlot 13; Systat Software, Inc., Chicago, IL, USA).

Specimens from each group were treated with the same methods and observed with a three-dimensional laser-scanning microscope (LSM; VK-8700; Keyence Corp., Osaka, Japan) (20,21).

Results

B-scan images of specimens obtained by OCT are shown in Fig. 2. The x-axis of each tomogram shows the scan depth, and the y-axis shows the vertical measurement position on the tooth surface. In the De group, a weak and narrow signal from the enamel surface, without any

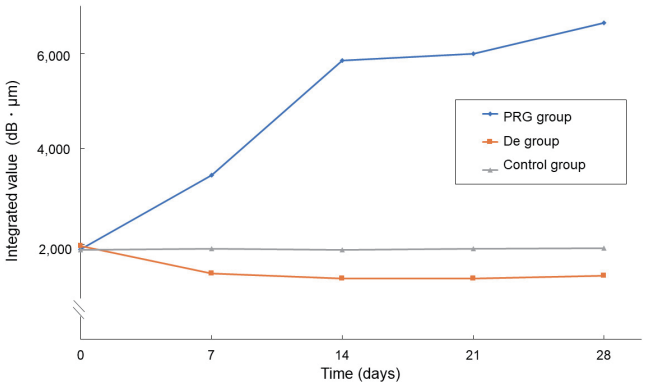

Fig. 3 Change in integrated values differed between groups. The Control and De groups exhibited small and nonsignificant increases in integrated values. Integrated values were higher in the PRG group at 7 days after the start of measurement and continued to increase thereafter.

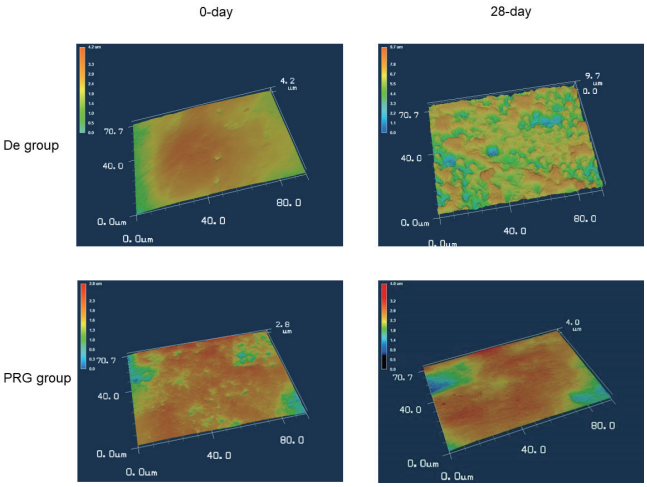

Fig. 4 Representative laser-scanning microscopy plan-view images of enamel surfaces. In the De group, acidic attack had caused pronounced morphologic changes in tooth surfaces after 28 days of treatment. However, the changes were minor in the PRG group.

Table 4 Effect of treatment procedure and duration on integrated values (dB·μm)

	Treatment time (days)				
Group	0	7	14	21	28
Control	1,884 (73.1) aA	1,908 (62.6) aC	1,884 (49.0) aC	1,904 (67.8) aC	1,916 (69.2) aC
De	1,964 (74.5) aA	1,386 (98.4) bB	1,284 (57.0) bB	1,284 (59.0) bB	1,340 (74.5) bB
PRG	1,888 (59.1) aA	3,454 (75.6) bA	5,859 (97.1) cA	6,003 (101) dA	6,642 (82.5) eA

De, Demineralization group; PRG, PRG filler extraction solution. Data are means (standard deviation). $n = 6$ per group. Values in the same group with the same lowercase letters indicate no significant difference ($P > 0.05$). For values in different groups at the same treatment time, means with the same uppercase letters are not significantly different ($P > 0.05$).

back-scattered intensity, was observed on Day 0, and little change was evident in OCT images during the 28-day test period. In the PRG group, visible signals from the enamel surface and back-scattered light were considerably above the noise level on Day 0, which caused a grainy appearance on OCT images. After 28 days, areas of weak scattering were observed on the enamel surface, and the back-scattered grainy appearance was weak.

Peak signal intensity (dB) and width at $1/e^2$ (μm) are shown in Tables 2 and 3. Although there were no significant changes in signal intensity or width at $1/e^2$ in the Control and De groups during the test period, significant changes were evident in the PRG group during the period from Day 0 to Day 7.

The integrated values (dB·μm) of each group are presented in Fig. 3, and changes in integrated values differed between groups (Table 4). The Control and De groups exhibited small and nonsignificant increases in integrated values. Seven days after the start of measurement, integrated values had increased in the PRG group and significantly increased thereafter.

Representative LSM images of enamel surfaces (Fig. 4) revealed morphologic differences caused by the various treatments. Although the Control and De groups did not significantly differ, pronounced morphologic changes were visible on the dentin surface of PRG group specimens.

Discussion

Like other calcified tissues, enamel has a characteristic hierarchic structure, which has an important effect on its optical properties (22). Hydroxyapatite crystallites, which are rectangular in cross-section, have a mean thickness of 26 nm and a mean width of 68 nm at the crystal level. Nano-sized crystallites are tightly packed in a distinct pattern and form keyhole-shaped rod units with a diameter of around 5 mm. These are surrounded by an organic-rich sheath at the rod-unit level. Permanent enamel contains about 2% w/w (around 6% v/v) water in free and bound forms (23). Changes in the water content of tooth enamel substantially alter its appearance, and decreased translucency was reported to be related to replacement of water around the enamel prisms as a result of air blowing (24).

OCT is a noninvasive imaging technique that uses near-infrared light to obtain information on subsurface

changes in specimens (25). The present OCT system uses low-coherence interferometry to measure echo time delay and the magnitude of back-scattered light reflected from specimens. Various phenomena occur during the interaction between a tooth and light flux, including light reflection at the surface, specular reflection at the surface, diffuse specular transmission of the light flux through the tooth, and scattering and absorption of the light flux within the tooth (26).

When attempting to measure lesion depth and severity, definition of the cutoff point is difficult because of the high dynamic range of reflectivity detected by OCT. The depth at which there is a ($1/e^2$) decrease in intensity can be used to determine cutoff values for intensity (27), and we used this calculation in our study. In addition, to define changes in the quantity of tooth substrate, we used the area of peak intensity to calculate the integrated value, signal intensity, and bandwidth at $1/e^2$. A previous study reported a significant positive correlation between lesion severity, as detected by transverse microradiography, and integrated reflectivity, in units of dB × μm, as detected by OCT (28). Consequently, the lower signal intensity and greater width at $1/e^2$ seen in the PRG group after 28 days indicated that light had traveled via a longer pathway than in the De group. Because of the release of ions from the PRG coating material, pores in the enamel surface may have accumulated minerals, thus changing its optical properties (29).

OCT images differentiate the optical properties of enamel substrates, including light absorption and light scattering (30). The perpendicular axis signal from enamel specimens was weakened by scattering and depolarization. After demineralization of the enamel substrates, the perpendicular axis signal was high because of intense depolarization caused by light scattering. Demineralization increases the roughness of enamel surfaces, thereby increasing light scattering by two to three orders. Therefore, a strong increase in the signal visible in B-scans indicates severe demineralization and roughening of the enamel surface (Fig. 2).

The present coating material containing S-PRG filler inhibited demineralization in the acid challenges. Several mechanisms explain the protective effects of the coating material. One of the most important is sealing of the enamel surface with a resinous layer containing inorganic fillers. This coating layer may act as a physical barrier against penetration of acidic solutions. However, the most important mechanism might be the pH-modulating effect of the S-PRG filler under acidic conditions, which can aid in protecting the enamel surface from acidic attack. One study found that S-PRG fillers neutralize their storage media (31). In addition, the coating material might enhance acid resistance of the enamel surface by taking up multiple ions released by the S-PRG filler (14).

Coating materials containing S-PRG filler were developed for their structural and ion-releasing properties. Si is important in mineralization of the tooth substrate, as it promotes hydroxyapatite formation by triggering hydroxyapatite nucleation in the presence of silica gel (32). In aqueous environments, sodium ions (Na^+) are rapidly exchanged with hydrogen cations (H^+ or H_3O^+) from the solution. Soluble silica in the form of $Si(OH_4)$ is lost into the solution after breakage of Si-O-Si bonds and formation of Si-OH (silanols) at the glass-solution interface. Migration of Ca^{2+} and PO_3^{4-} groups to calcium sodium phosphosilicate particles through the SiO_2^--rich surface causes formation of a CaO-P_2O_5-rich film on particle surfaces, which then crystallizes into hydroxycarbonate apatite (33). Si released from bioactive glass is thought to adhere to the substance, thus providing sites for heterogeneous CaP nucleation (34). Once nucleation occurs, spontaneous growth continues in the solution, thereby yielding a bone-like apatite layer that arrests caries in primary enamel.

Adhesive systems have been suggested as an effective measure to protect exposed dentin structures from acidic attack (35). Despite encouraging results showing reductions in the severity of carious lesions, adhesive coatings cannot fully protect against demineralization induced by acidic attack (36), perhaps because the presence of hydrophilic monomers makes some one-step self-etching adhesives permeable to water (37). Thus, there is a need for new coating materials that can effectively protect the tooth surface from chemical and biological attacks. The present coating material comprises base and active liquids and can release multiple ions, including F^-, Al^{3+}, B^-, and Sr^{2+}, which have an anti-demineralization effect on underlying and adjacent enamel (38). In addition to their remineralization ability, S-PRG filler-containing resins inhibit plaque formation (39,40). This coating material is easily applied to the tooth surface and may help prevent acidic attack in children and persons with poor oral hygiene.

In this study, OCT was successfully used to track remineralization and test the ability of a coating material containing S-PRG filler to inhibit demineralization. Within the limitations of this study, the null hypothesis—that the coating material would not affect the structural condition of artificially demineralized primary tooth enamel—was rejected. In clinical settings, coating materials containing S-PRG filler might help prevent demineralization of primary tooth enamel.

Acknowledgments

This work was supported, in part, by a Grant-in-Aid for Scientific Research (C) (15K11130, 16K11564, 17K11716) and a Grant-in-Aid for Young Scientists (B) (17K17140, 17K17142) from the Japan Society for the Promotion of Science, and by the Sato Fund, Nihon University School of Dentistry, Japan.

Conflict of interest

The authors affirm that they have no proprietary, financial, or other personal interest of any nature in any product, service, or company presented in this article.

References

1. Boyce WT, Den Besten PK, Stamperdahl J, Zhan L, Jiang Y, Adler NE et al. (2010) Social inequalities in childhood dental caries: the convergent roles of stress, bacteria and disadvantage. Soc Sci Med 71, 1644-1652.
2. Costa FS, Silveira ER, Pinto GS, Nascimento GG, Thomson WM, Demarco FF (2017) Developmental defects of enamel and dental caries in the primary dentition: a systematic review and meta-analysis. J Dent 60, 1-7.
3. Chou R, Cantor A, Zakher B, Mitchell JP, Pappas M (2013) Preventing dental caries in children <5 years: systematic review updating USPSTF recommendation. Pediatrics 132, 332-350.
4. Maher L, Phelan C, Lawrence G, Torvaldsen S, Dawson A, Wright C (2012) The early childhood oral health program: promoting prevention and timely intervention of early childhood caries in NSW through shared care. Health Promot J Austr 23, 171-176.
5. O'Mullane DM, Baez RJ, Jones S, Lennon MA, Petersen PE, Rugg-Gunn AJ et al. (2016) Fluoride and oral health. Community Dent Health 33, 69-99.
6. Shiiya T, Mukai Y, Tomiyama K, Teranaka T (2012) Anti-demineralization effect of a novel fluoride-releasing varnish on dentin. Am J Dent 25, 347-350.
7. Ma S, Imazato S, Chen JH, Mayanagi G, Takahashi N, Ishimoto T et al. (2012) Effects of a coating resin containing S-PRG filler to prevent demineralization of root surfaces. Dent Mater J 31, 909-915.
8. Ikemura K, Tay FR, Kouro Y, Endo T, Yoshiyama M, Miyai K et al. (2003) Optimizing filler content in an adhesive system containing pre-reacted glass-ionomer fillers. Dent Mater 19, 137-146.
9. Ikemura K, Tay FR, Endo T, Pashley DH (2008) A review of chemical-approach and ultramorphological studies on the development of fluoride-releasing dental adhesives comprising new pre-reacted glass ionomer (PRG) fillers. Dent Mater J 27, 315-339.
10. Fujimoto Y, Iwasa M, Murayama R, Miyazaki M, Nagafuji A, Nakatsuka T (2010) Detection of ions released from S-PRG fillers and their modulation effect. Dent Mater J 29, 392-397.
11. Han L, Okiji T (2011) Evaluation of the ions release/incorporation of the prototype S-PRG filler-containing endodontic sealer. Dent Mater J 30, 898-903.
12. Thuy TT, Nakagaki H, Kato K, Hung PA, Inukai J, Tsuboi S et al. (2008) Effect of strontium in combination with fluoride on enamel remineralization in vitro. Arch Oral Biol 53, 1017-1022.
13. Yassen GH, Lippert F, Eckert G, Eder J, Zandoná AF (2012) The effect of strontium and combinations of strontium and fluoride on the remineralization of artificial caries lesions in vitro. Quintessence Int 43, e95-103.
14. Kaga M, Kakuda S, Ida Y, Toshima H, Hashimoto M, Endo K et al. (2014) Inhibition of enamel demineralization by buffering effect of S-PRG filler-containing dental sealant. Eur J Oral Sci 122, 78-83.
15. Murayama R, Furuichi T, Yokokawa M, Takahashi F, Kawamoto R, Takamizawa T et al. (2012) Ultrasonic investigation of the effect of S-PRG filler-containing coating material on bovine tooth demineralization. Dent Mater J 31, 954-959.
16. Hosoya Y, Ando S, Otani H, Yukinari T, Miyazaki M, Garcia-Godoy F (2013) Ability of barrier coat S-PRG coating to arrest artificial enamel lesions in primary teeth. Am J Dent 26, 286-290.
17. Rochlen GK, Wolff MS (2011) Technological advances in caries diagnosis. Dent Clin North Am 55, 441-452.
18. Louie T, Lee C, Hsu D, Hirasuna K, Manesh S, Staninec M et al. (2010) Clinical assessment of early tooth demineralization using polarization sensitive optical coherence tomography. Lasers Surg Med 42, 738-745.
19. Abogazalah N, Ando M (2017) Alternative methods to visual and radiographic examinations for approximal caries detection. J Oral Sci 59, 315-322.
20. Kotaku M, Murayama R, Shimamura Y, Takahashi F, Suzuki T, Kurokawa H et al. (2014) Evaluation of the effects of fluoride-releasing varnish on dentin demineralization using optical coherence tomography. Dent Mater J 33, 648-655.
21. Iino M, Murayama R, Shimamura Y, Kurokawa H, Furuichi T, Suzuki T et al. (2014) Optical coherence tomography examination of the effect of S-PRG filler extraction solution on the demineralization of bovine enamel. Dent Mater J 33, 48-53.
22. He LH, Swain MV (2008) Understanding the mechanical behaviour of human enamel from its structural and compositional characteristics. J Mech Behav Biomed Mater 1, 18-29.
23. Dibdin GH (1993) The water in human dental enamel and its diffusional exchange measured by clearance of tritiated water from enamel slabs of varying thickness. Caries Res 27, 81-86.
24. Brodelt RHW, O'Brien WJ, Fan PL, Frazer-Dib JG, Yu R (1981) Translucency of human dental enamel. J Dent Res 60, 1749-1753.
25. Fercher AF (2010) Optical coherence tomography--development, principles, applications. Z Med Phys 20, 251-276.
26. Karlsson L (2010) Caries detection methods based on changes in optical properties between healthy and carious tissue. Int J Dent 2010, 270279.
27. Can AM, Darling CL, Ho C, Fried D (2008) Non-destructive

assessment of inhibition of demineralization in dental enamel irradiated by a λ=9.3-μm CO_2 laser at ablative irradiation intensities with PS-OCT. Lasers Surg Med 40, 342-349.
28. Manesh SK, Darling CL, Fried D (2009) Nondestructive assessment of dentin demineralization using polarization-sensitive optical coherence tomography after exposure to fluoride and laser irradiation. J Biomed Mater Res B Appl Biomater 90, 802-812.
29. Kang H, Darling CL, Fried D (2012) Nondestructive monitoring of the repair of enamel artificial lesions by an acidic remineralization model using polarization-sensitive optical coherence tomography. Dent Mater 28, 488-494.
30. Colston BW, Sathyam US, DaSilva LB, Everett MJ, Stroeve P, Otis LL (1998) Dental OCT. Opt Express 3, 230-238.
31. Itota T, Al-Naimi OT, Carrick TE, Yoshiyama M, McCabe JF (2005) Fluoride release and neutralizing effect by resin-based materials. Oper Dent 30, 522-527.
32. Radin S, Ducheyne P, Rothman B, Conti A (1997) The effect of in vitro modeling conditions on the surface reactions of bioactive glass. J Biomed Mater Res 37, 363-375.
33. Andersson ÖH, Kangasniemi I (1991) Calcium phosphate formation at the surface of bioactive glass in vitro. J Biomed Mater Res 25, 1019-1030.
34. Tanahashi M, Yao T, Kokubo T, Minoda M, Miyamoto T, Nakamura T et al. (1994) Apatite coated on organic polymers by biomimetic process: improvement in its adhesion to substrate by NaOH treatment. J Appl Biomater 5, 339-347.
35. Guan R, Takagaki T, Matsui N, Sato T, Burrow MF, Palamara J et al. (2016) Dentin bonding performance using Weibull statistics and evaluation of acid-base resistant zone formation of recently introduced adhesives. Dent Mater J 35, 684-693.
36. Gernhardt CR, Koravu T, Gerlach R, Schaller HG (2004) The influence of dentin adhesives on the demineralization of irradiated and non-irradiated human root dentin. Oper Dent 29, 454-461.
37. Tay FR, Frankenberger R, Krejci I, Bouillaguet S, Pashley DH, Carvalho RM et al. (2004) Single-bottle adhesives behave as permeable membranes after polymerization. I. In vivo evidence. J Dent 32, 611-621.
38. Shimazu K, Ogata K, Karibe H (2011) Evaluation of the ion-releasing and recharging abilities of a resin-based fissure sealant containing S-PRG filler. Dent Mater J 30, 923-927.
39. Saku S, Kotake H, Scougall-Vilchis RJ, Ohashi S, Hotta M, Horiuchi S et al. (2010) Antibacterial activity of composite resin with glass-ionomer filler particles. Dent Mater J 29, 193-198.
40. Hahnel S, Wastl DS, Schneider-Feyrer S, Giessibl FJ, Brambilla E, Cazzaniga G et al. (2014) Streptococcus mutans biofilm formation and release of fluoride from experimental resin-based composites depending on surface treatment and S-PRG filler particle fraction. J Adhes Dent 16, 313-321.